Controllable Supramolecular Assembly by $\pi-\pi$ Interactions: Cobalt(II) and Copper(II) Complexes with Benzimidazole Derivatives

Wen-Hua Sun,*[,†] Changxing Shao,[†] Yong Chen,[†] Huaiming Hu,[†] Roger A. Sheldon,[‡] Honggen Wang,[§] Xuebing Leng,[§] and Xianglin Jin[⊥]

State Key Laboratory of Engineering Plastics and The Center for Molecular Science, Institute of Chemistry, The Chinese Academy of Sciences, Beijing 100080, China, Department of Biotechnology, Faculty of Applied Sciences, Delft University of Technology, 2600 GA Delft, The Netherlands, State Key Laboratory of Functional Polymer, Nankai University, Tianjin 300071, China, and Institute of Physical Chemistry, Peking University, Beijing 100871, China

Received May 8, 2002

Two novel helical supramolecular architectures were constructed by self-assembly of cobalt(II) (**1**) and copper(II) complexes (**2**) of 1-[(5-methyl-2-furyl)methylene]-2-(5-methyl-2-furyl)benzimidazole in the crystalline form, which were stabilized through the intra- and intermolecular $\pi-\pi$ interactions between benzimidazole rings. When the methylfuran fragment of the ligand was switched to a furan group, the cobalt complex (**3**) of 1-(2-furylmethylene)-2-(2-furyl)benzimidazole formed another type of supramolecular network through $\pi-\pi$ interactions under similar reaction conditions. The spectral and thermal behaviors of complexes **1**−**3** were investigated by ultraviolet, chiral dichroism, and fluorescence spectral and thermogravimetric techniques. When MAO was used as the cocatalyst, complex **1** displayed satisfactory activity for ethylene oligomerization up to 2.5 $\times$ 10^5 g of C_2H_4 mol^{-1} h^{-1} at room temperature and 9 atm of ethylene.

Introduction

New multidimensional supramolecular networks with well-defined structures assembled from organic molecules and metal-ion building blocks are currently of much interest in chemistry and materials science.[1] It has been demonstrated that one of the most important features of such supramolecular architectures is the simultaneous operation of several weak interactions between building blocks, such as hydrogen bonding, $\pi-\pi$, and metal−ligand interactions.[2] Among the intermolecular interactions, noncovalent interactions between aromatic rings are of particular importance in controlling the stacking of aromatic molecules in the crystalline state as well as the conformational preferences and development of supramolecular assemblies.[3−6] Although the phenomenon of $\pi-\pi$ interactions in aromatic compounds has been known for several decades, it has recently attracted considerable interest because of its relevance to DNA, proteins, and other biological systems.[7,8] Among the various families of organic ligands, benzimidazoles have recently attracted considerable interest for their wide-ranging antiviral activity and the possibility of forming supramolecular aggregates with transition-metal ions. During the past few decades, a number of structural investigations related to the copper(II) and cobalt(II) halide complexes with benzimidazoles have been reported.[9−14] Herein, we report the formation of three novel, self-assembling supramolecular aggregates from cobalt and copper complexes of 1-[(5-methyl-2-furyl)methylene]-2-(5-methyl-2-furyl)benzimidazole (**L1**) and 1-[2-furylmethylene]-2-(2-furyl)benzimidazole (**L2**) as building blocks, by extensive intra- and intermolecular $\pi-\pi$ stacking. The special interest of these complexes is their helical array or supramo-

* To whom correspondence should be addressed. E-mail: whsun@infoc3.icas.ac.cn.
† Institute of Chemistry, The Chinese Academy of Sciences.
‡ Delft University of Technology.
§ Nankai University.
⊥ Peking University.

(1) Piguet, C.; Bernardinelli, G.; Hepfgartner, G. *Chem. Rev.* **1997**, *97*, 2005.
(2) (a) Leinnger, S.; Olenyuk, B.; Stang, P. J. *Chem. Rev.* **2000**, *100*, 853. (b) Conn, M. M.; Rebek, J. J. *Chem. Rev.* **1997**, *97*, 1647. (c) Müller-Dethlefs, K.; Hobza, P. *Chem. Rev.* **2000**, *100*, 143.
(3) Childs, L. J.; Alcock, H. W.; Hannon, M. J. *Angew. Chem., Int. Ed.* **2001**, *40*, 1079.
(4) Blake, A. J.; Champness, N. R.; Khlobystov, A. N.; Parsons, S.; Schröder, M. *Angew. Chem., Int. Ed.* **2000**, *39*, 2317.
(5) Min, K. S.; Suh, M. P. *Eur. J. Inorg. Chem.* **2001**, 449.
(6) (a) Jorgensen, W. L.; Severance, D. L. *J. Am. Chem. Soc.* **1990**, *112*, 4768. (b) Abrahams, B. F.; Jackson, P. A.; Robson, R. *Angew. Chem., Int. Ed.* **1998**, *37*, 2656.
(7) (a) Hunter, C. A.; Sanders, J. K. M. *J. Am. Chem. Soc.* **1990**, *112*, 5525. (b) Hobza, P.; Selzle, H. L.; Schlag, E. W. *J. Am. Chem. Soc.* **1994**, *116*, 3500.
(8) (a) Zielinski, W. S.; Orgel, L. E. *Nature* **1987**, *327*, 346. (b) O'Neil, K. T.; Hoess, R. H.; Degrado, W. F. *Science* **1990**, *249*, 774.
(9) Sundberg, R. J.; Yilmaz, I.; Mente, D. C. *Inorg. Chem.* **1977**, *16*, 1470.
(10) Belicchi, M. F.; Gasparri, G. F.; Pelizzi, C.; Tarasconi, P. *Transition Met. Chem.* **1985**, *10*, 295.
(11) van Albada, G. A.; Smeets, W. J. J.; Spek, A. L.; Reedijk, J. *Inorg. Chim. Acta* **1999**, *288*, 220.
(12) Shan, Y.; Cádiz, M. E.; Sánchez, P. L.; Huang, S. D. *Acta Crystallogr., Sect. C* **1999**, *55*, 1262.
(13) (a) Bukowska-Strzyzewska, M.; Tosik, A. *J. Crystallogr. Spectrosc. Res.* **1991**, *21*, 379. (b) Bukowska-Strzyzewska, M.; Tosik, A. *J. Crystallogr. Spectrosc. Res.* **1988**, *18*, 525.
(14) (a) Sokol, V. I.; Porai-Koshits, M. A.; Davydov, V. V.; Zaitsev, B. E.; Palishkin, M. V.; Kukalenko, S. S. *Zh. Neorg. Khim.* **1989**, *34*, 884. (b) Sokol, V. I.; Davydov, V. V.; Porai-Koshits, M. A.; Zaitsev, B. E.; Palishkin, M. V.; Kukalenko, S. S. *Zh. Neorg. Khim.* **1989**, *34*, 2573.

10.1021/om020370r CCC: $22.00
Publication on Web 08/31/2002

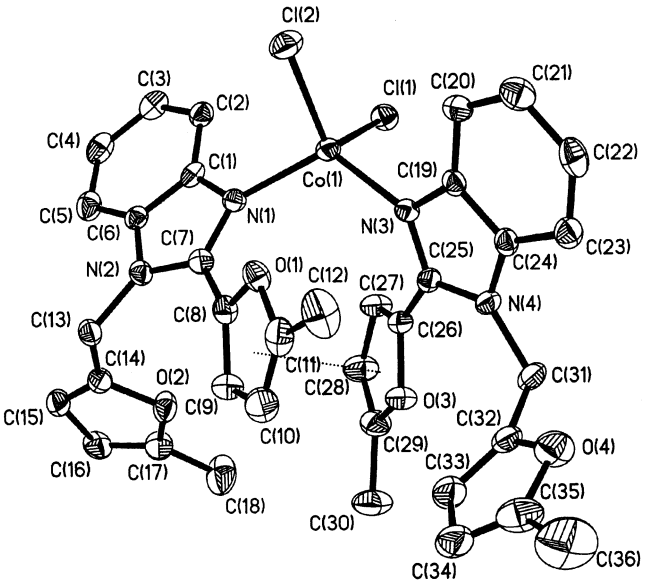

Figure 1. Thermal ellipsoid plot of complex **1** (the dotted line indicates the $\pi-\pi$ interaction).

Scheme 1. Syntheses of the Title Complexes

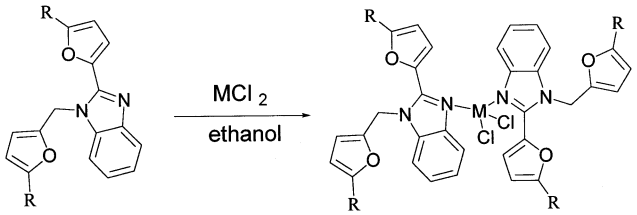

lecular network, achieved by slightly tuning the substituents of the ligands.

Results and Discussion

Ligands **L1** and **L2** were synthesized by the reaction of *o*-phenylenediamine with 5-methyl-2-furaldehyde and furfural, respectively. Their subsequent reactions with cobalt or copper dichloride gave the corresponding title complexes in yields of higher than 80% (Scheme 1). An ORTEP drawing of the complex **1** is shown in Figure 1. The cobalt adopts a four-coordinate distorted-tetrahedral environment by two nitrogen atoms at the 3-position of the benzimidazole moieties and two terminal chlorine atoms with cis angles in the range of 102.15−118.03°. Intramolecular $\pi-\pi$ interactions between two methylfuran rings at the 2-positions of the benzimidazole ligands (centroid distance 3.5190(12) Å, dihedral angle 9.1°) further stabilized this conformation.

It is noteworthy that, as can be seen in parts a and b of Figure 2, each of the benzimidazole units of the complex **1** tightly overlaps with the respective benzimidazole ring of another complex with the identical distance of 3.4749(10) Å and dihedral angle of 0°. On the other hand, two benzimidazole groups in a single complex are located at a dihedral angle of 52.0°. These interconnections consequently enabled the complex monomers to form a unique self-assembling supramolecular helix in the solid state through the intermolecular $\pi-\pi$ stacking.

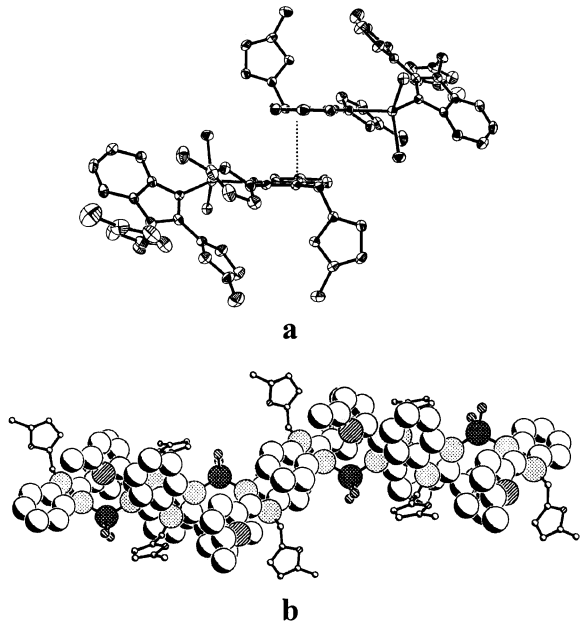

Figure 2. Side views of assembly by complex **1** from different angles (the dotted line indicates the $\pi-\pi$ interaction).

By switching the central cobalt ion of complex **1** to a copper ion, we obtained an analogous but loose supramolecular helix assembled by complex **2** (Figure 3). Compared with complex **1** (Figure 4), the dihedral angle between two intramolecular benzimidazole rings of the complex **2** decreased to 29.9°, while the centroid distance between two intermolecular benzimidazoles increased to 3.5868(9) Å with a dihedral angle of 0°. This reveals that the coordinating behavior of the cobalt and copper complexes differs to some extent. Further evidence was obtained from the UV−vis spectra. In comparison with the original absorption spectrum of ligand **L1**, which displays a characteristic peak at 313 nm ($\epsilon = 2.2 \times 10^4$ M^{-1} cm^{-1}), the ϵ value of its cobalt complex **1** significantly increased to 1.14×10^5 M^{-1} cm^{-1}, while the copper complex **2** gave an ϵ value of 4.3×10^4 M^{-1} cm^{-1}. Further, upon coordination with ligand **L1**, the irreversible oxidation potential of $CoCl_2$ displayed a more significant decrease (1.822 to 1.564 V) than $CuCl_2$ (0.999 to 0.940 V). These results infer that ligand coordination in the complex **1** is stronger than in complex **2**.

Interestingly, the cobalt complex with **L2** shows a noticeably different conformation as compared to its analogue with ligand **L1** (Figure 5). Two nitrogen atoms on the benzimidazole rings and two terminal chlorine atoms are coordinated to the metal center with the cis angles in the range of 107.03−113.40°, and the intramolecular $\pi-\pi$ interactions between the two methylfuran rings at the 2-positions of the benzimidazole ligands change to the interaction between the furan ring and benzimidazole group (centroid distance 3.4952(10) Å and dihedral angle 24.3°). C14a, C14b, C15a, and C15b are disordered. The dihedral angle between two benzimidazole groups is 55.5°, which is larger than that in complex **1**. In addition, the Co−N bonds (2.022(4) Å) are shorter than those in complex **1** (2.050(3) and 2.061(3) Å), which indicates a stronger coordination between the cobalt and the ligand **L2**. The UV spectra show that, compared with the original absorption spectrum of ligand **L2**, which displays a characteristic peak at 296

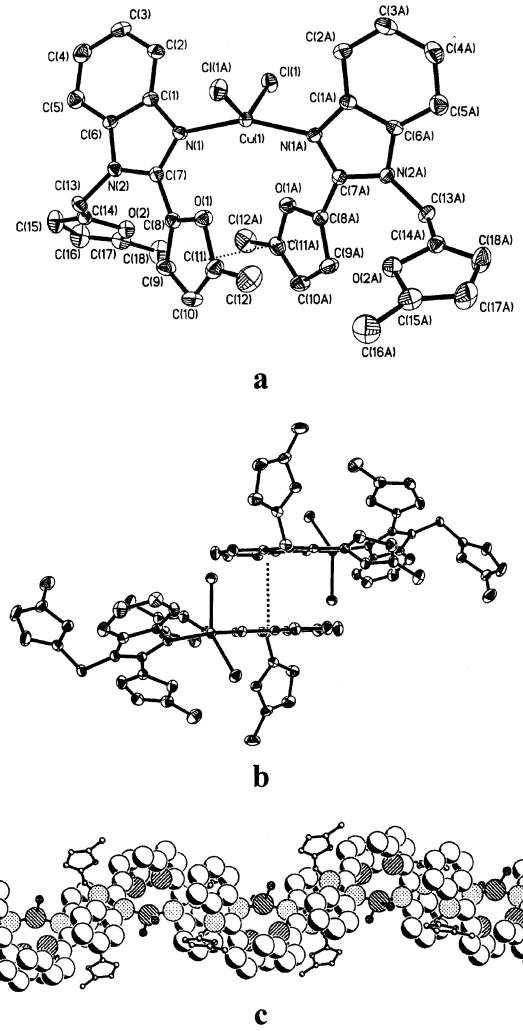

Figure 3. (a) Thermal ellipsoid plot of complex **2** (centroid distance between two 2-position methylfuran rings 3.4047 Å, dihedral angle 7.4°). (b) Side view of the copper assembly (the dotted lines indicate the $\pi-\pi$ interactions). (c) Helical complex polymer.

nm ($\epsilon = 3.95 \times 10^4$ M^{-1} cm^{-1}), the ϵ value of cobalt complex **3** was significantly enhanced to 6.32×10^5 M^{-1} cm^{-1} with an obvious bathochromic shift (12.7 nm) of the relevant peak. Furthermore, upon coordination with ligand **L2**, the irreversible oxidation potential of $CoCl_2$ displayed a more remarkable decrease (0.5 V) than with ligand **L1**.

Moreover, unlike complexes **1** and **2**, which assemble into the one-dimensional helical structure through intermolecular $\pi-\pi$ stacking between the benzimidazole groups of the neighboring molecules, the cobalt complex **3** aggregates to a two-dimensional superamolecular network (Figure 6) in the solid state through the intermolecular $\pi-\pi$ stacking between the furan ring and the benzimidazole group of the adjacent complex moiety (centroid distance 3.1261(10) Å and dihedral angle 9.3°). In all probability, this was caused by changing the methylfuran group of the ligand to a furan group. This phenomenon may be attributed to the fact that, as compared with the bulky methylfuran group, the furan group comes closer to the benzimidazole group in a shorter distance, leading to more efficient $\pi-\pi$ interactions.

The crystallographic data for complexes **1**−**3** is listed in Table 1, and selected bond distances and angles are presented in Table 2. From these tables, it is clearly evident that the complexes synthesized are crystalline in nature.

To study the thermal stability of the different self-assemblies constructed by the same metal and different ligands, the complexes **1** and **3** were investigated by thermogravimetric (TG) techniques. As shown in Figure 7, the complex **3** displays two decomposition peaks at 250 and 500 °C, respectively (Figure 7a), and the first decomposition temperature of complex **3** is higher than the corresponding value (220 °C) of complex **1** (Figure 7b). The higher decomposition temperature indicates that complex **3** is more stable due to the strong inter- and intramolecular $\pi-\pi$ interactions, and the strong coordination interaction between cobalt and ligand **L2**, which is confirmed by the shorter Co−N bond length in complex **3**.

At room temperature, the CD spectra (Figure 8) of complexes **1**−**3** in $CHCl_3$ display their chirality and relative Cotton effect. The CD spectrum of ligand **L1** shows a very weak positive Cotton effect at 345 nm ($\Delta\epsilon = +0.0241$ dm^3 mol^{-1} cm^{-1}). Upon coordination with

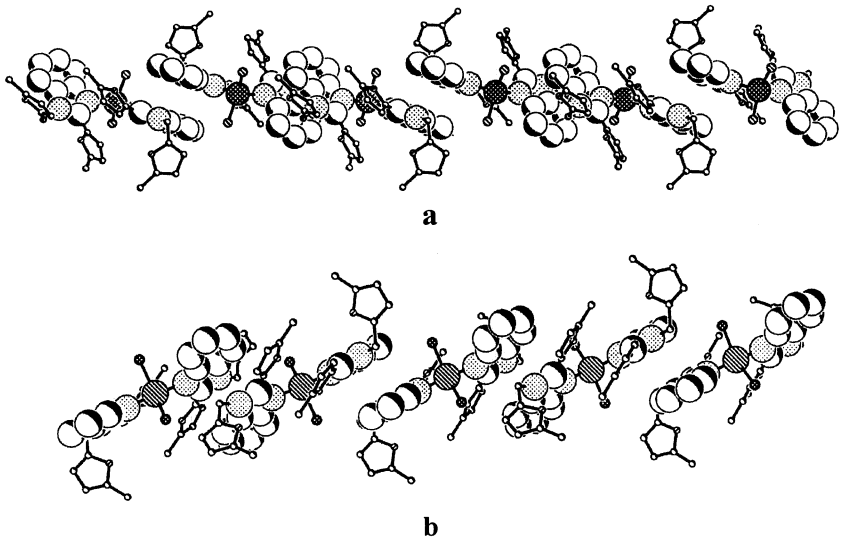

Figure 4. Comparative side views of helical complex polymers by complex **1** (a) and by complex **2** (b).

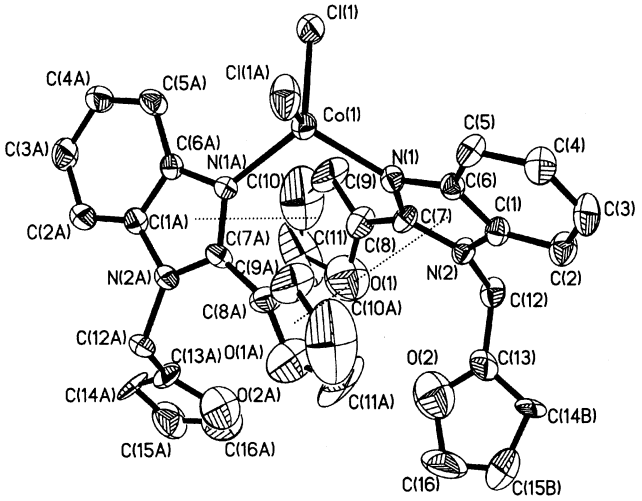

Figure 5. Thermal ellipsoid plot of complex **3** (the dotted line indicates the π−π interaction).

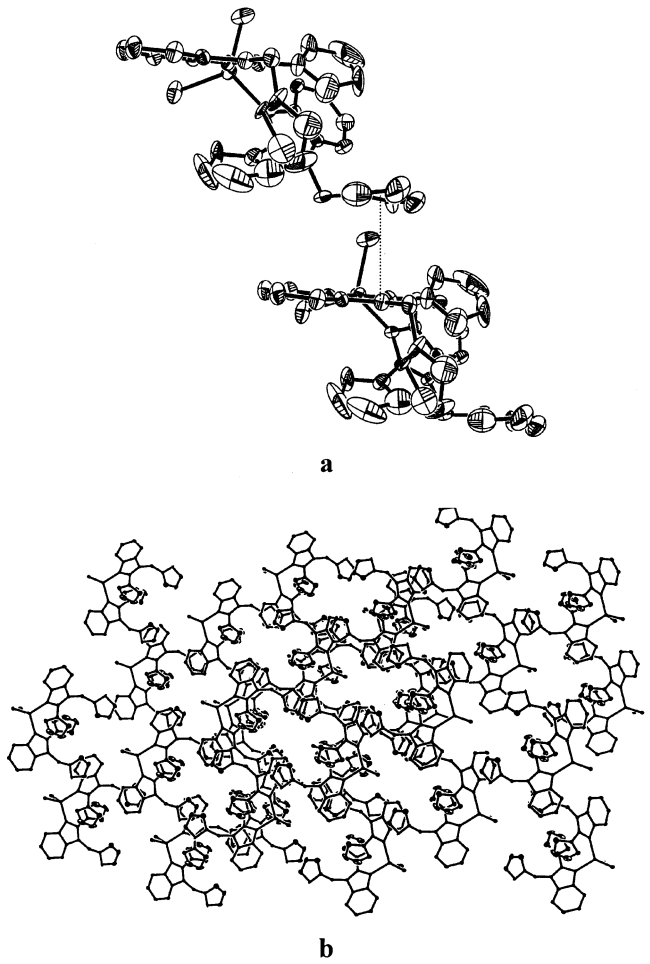

Figure 6. Side views of assembly by complex **3** from different angles (the dotted line indicates the π−π interaction).

metal ion, the Δε value of the relevant Cotton effect is clearly enhanced to 0.0329 dm^3 mol^{-1} cm^{-1} (341 nm) for **1** and 0.0833 dm^3 mol^{-1} cm^{-1} (338 nm) for **2**, accompanying the appearance of an additional negative band at 321 nm (−0.0517 dm^3 mol^{-1} cm^{-1}) for **1** and 338 nm (−0.0216 dm^3 mol^{-1} cm^{-1}) for **2**, respectively (Figure 8a). However, for complex **3**, the CD spectrum displays a fairly large positive Cotton effect, and the observed Δε values are +7.8229 dm^3 mol^{-1} cm^{-1} (324 nm), +11.7773 dm^3 mol^{-1} cm^{-1} (276.5 nm), +15.9168 dm^3 mol^{-1} cm^{-1} (241.4 nm), and +18.8863 dm^3 mol^{-1} cm^{-1} (218.3 nm). (Figure 8b). In addition to the CD spectra, the fluorescence spectra of complexes **1**−**3** have been recorded at a concentration of 2.5×10^{-5} mol dm^{-3} and compared with those of the parent ligands. As can be seen in Figure 9, both the cobalt complexes **1** and **3** show analogous, but obviously weak, fluorescence signals as compared with the uncoordinated ligands **L1** and **L2**. Surprisingly, however, the relative fluorescence intensity of ligand **L1** is appreciably enhanced upon association with copper ion. This opposite trend of the fluorescence phenomenon of ligand **L1** upon ligating

Table 1. Crystallographic Data for Complexes 1−3

	1	**2**	**3**
chem formula	$C_{36}H_{32}Cl_2CoN_4O_4$	$C_{36}H_{32}Cl_2CuN_4O_4$	$C_{32}H_{24}Cl_2CoN_4O_4$
cryst size (mm)	0.25 × 0.20 × 0.15	0.30 × 0.20 × 0 .10	0.32 × 0.32 × 0.04
fw	714.49	719.10	658.38
temp (K)	293 ± 2	293 ± 2	293 ± 2
cryst syst	triclinic	monoclinic	monoclinic
space group	*P*1̄	*C*2/*c*	*C*2/*c*
unit cell params			
a (Å)	10.664(3)	22.150(6)	15.592(3)
b (Å)	10.884(3)	9.363(3)	11.115(2)
c (Å)	16.680(5)	17.882(5)	18.439(4)
α (deg)	75.154(5)	90	90
β (deg)	77.856(5)	115.561(5)	111.89(3)
γ (deg)	66.430(5)	90	90
V (Å^3)	1699.4(8)	3345.3(17)	2965.2(10)
Z	2	4	4
no. of rflns measd	6984	6706	12749
no. of unique rflns	5907	2952	3389
no. of observns ($I \geq 2\sigma(I)$)	3144	1898	812
no. of params	424	213	202
R^a	0.0510	0.0395	0.0547
$R_w{}^b$	0.0736	0.0714	0.1016
S	0.957	0.958	0.626
$(\Delta/\sigma)_{max}$	0.001	0.004	0.018
max (min) resid density (e/Å^3)	0.321 (−0.397)	0.416 (−0.299)	0.296 (−0.254)

^{a} $R = \Sigma||F_o| - |F_c||/\Sigma|F_o|$. ^{b} $R_w = \{\Sigma w(|F_o| - |F_c|)^2/\Sigma wF_o{}^2\}^{1/2}$.

Table 2. Selected Bonds (Å) and Angles (deg) for Complexes 1−3

		Complex **1**	
Co(1)−N(1)	2.050(3)	Co(1)−N(3)	2.061(3)
Co(1)−Cl(2)	2.2687(15)	Co(1)−Cl(1)	2.2720(13)
N(1)−Co(1)−N(3)	118.03(13)	N(1)−Co(1)−Cl(2)	102.15(10)
N(3)−Co(1)−Cl(2)	113.96(10)	N(1)−Co(1)−Cl(1)	108.92(10)
N(3)−Co(1)−Cl(1)	103.73(9)	Cl(2)−Co(1)−Cl(1)	110.03(5)
C(7)−N(1)−Co(1)	132.3(3)	C(1)−N(1)−Co(1)	122.9(3)
C(25)−N(3)−Co(1)	129.1(3)	C(19)−N(3)−Co(1)	124.5(3)
		Complex **2**	
Cu(1)−N(1A)	1.988(2)	Cu(1)−N(1)	1.988(2)
Cu(1)−Cl(1)	2.2666(10)	Cu(1)−Cl(1A)	2.2666(10)
N(1A) −Cu(1)−N(1)	156.95(14)	N(1A) −Cu(1)−Cl(1)	93.52(7)
Cl(1)−Cu(1)−Cl(1)	95.70(7)	N(1A) −Cu(1)−Cl(1A)	95.70(7)
N(1)−Cu(1)−Cl(1A)	93.52(7)	Cl(1)−Cu(1)−Cl(1A)	132.61(6)
C(7)−N(1)−Cu(1)	128.7(2)	C(1)−N(1)−Cu(1)	125.0(2)
C(7)−N(1)−Cu(1)	128.7(2)	C(1)−N(1)−Cu(1)	125.0(2)
		Complex **3**	
Co(1)−N(1)	2.022(4)	Co(1)−N(1A)	2.022(4)
Co(1)−Cl(1A)	2.2517(18)	Co(1)−Cl(1)	2.2517(18)
N(1)−Co(1)−N(1A)	107.3(2)	N(1)−Co(1)−Cl(1A)	113.40(13)
N(1A)−Co(1)−Cl(1A)	107.03 (12)	N(1)−Co(1)−Cl(1)	107.03(12)
N(1A)−Co(1)−Cl(1)	113.40(13)	Cl(1A)−Co(1)−Cl(1)	108.82(11)
C(7)−N(1)−Co(1)	129.2(4)	C(6)−N(1)−Co(1)	126.1(3)

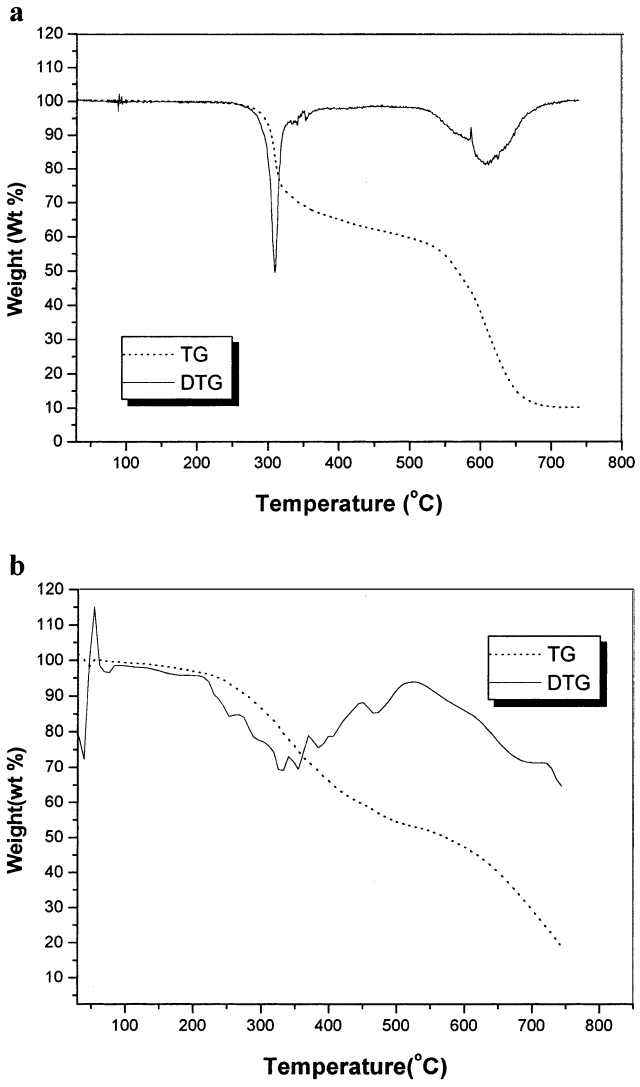

Figure 7. TG-DTG curves for the thermal decomposition of complex **3** (a) and complex **1** (b) under a nitrogen atmosphere at a heating rate of 10 °C/min.

with cobalt and copper ions may also arise from its different coordination behavior with these two ions to some extent, consequently enabling it to be a fluorescence probe for detecting transition-metal ions.

It is worth noting that these complexes are efficient catalysts for ethylene oligomerization. For example, complex **1** can oligomerize ethylene to give products distributed from C_4 to C_{20}, and the activity reached 2.5 $\times$ 10^5 g of C_2H_4 mol^{-1} h^{-1} at room temperature and 9 atm of ethylene with MAO as the cocatalyst (Al/Co = 500). When the Al/Co molar ratio was lowered to 250, the activity dramatically decreased to 9.8 $\times$ 10^3 g of C_2H_4 mol^{-1} h^{-1} at ambient temperature and the same ethylene pressure. The products that resulted were mainly the C_4 and C_6 species, along with a small amount of C_8. Compared with complex **1**, complex **3** only showed a marginal activity under the same catalytic conditions. When the Al/Co ratio is increased to 1000, the activity of complex **1** increases to 4.4 $\times$ 10^5 g of C_2H_4 mol^{-1} h^{-1}, and the products are C_4 and C_6 species. However, the copper complex **2** showed no catalytic activity for ethylene oligomerization or polymerization.

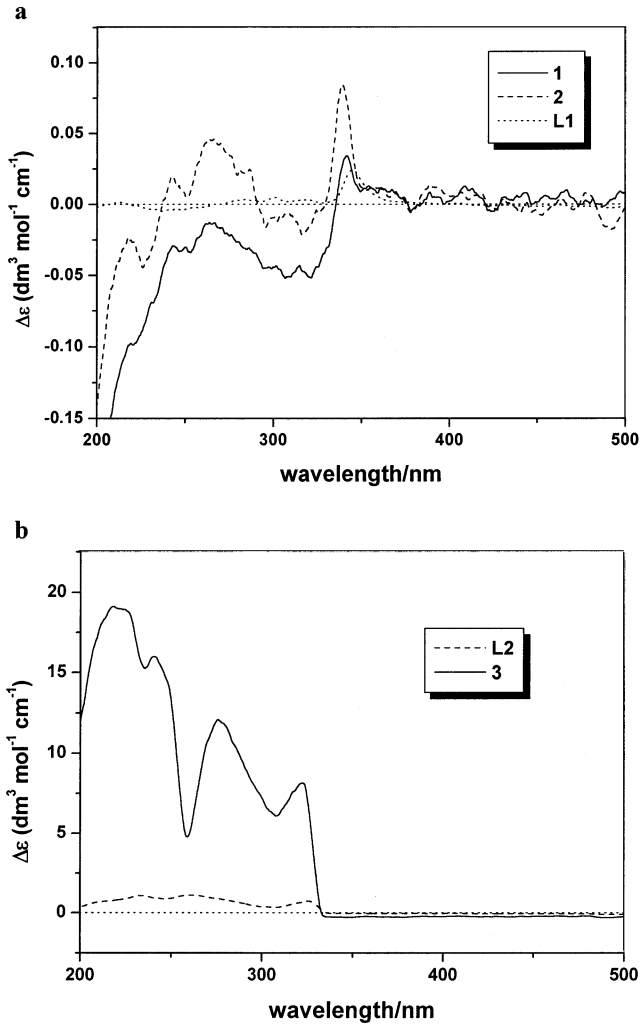

Figure 8. Circular dichroism spectra for ligand **L1** and complexes **1** and **2** (a) and for ligand **L2** and complex **3** (b) in $CHCl_3$.

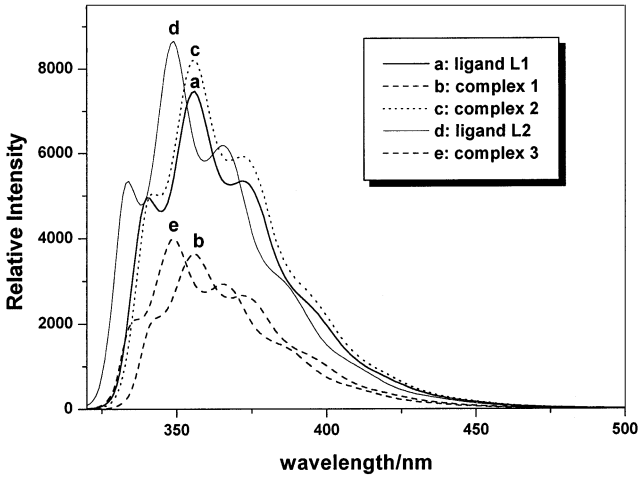

Figure 9. Fluorescence spectra of ligands **L1** and **L2** and complexes **1**−**3** in $CHCl_3$ (excitation wavelength 313 nm).

In summary, we confirmed the evidence for the formation of two helical and one netlike supramolecular assembly. The structural features and operative modes of the intra- and intermolecular $\pi-\pi$ interactions observed may be comparable with some highly ordered structures found in biological systems, such as globu-

lar[15] and cysteine proteins,[16] and could form the basis for designing novel supramolecular assemblies.

Experimental Section

Materials and Apparatus. All starting materials were commercially available from Acros and used without further purification. Solvents were refluxed over an appropriate drying agent and distilled prior to use. 1-(2-Furylmethylene)-2-(2-furyl)benzimidazole was prepared according to an established procedure.[17] Elemental analyses were performed by the Carlo Erba 1106 microanalytical service. NMR spectra were recorded on a Bruker spectrometer DMX-300 with TMS as the internal standard. Mass spectra were measured on a Kratos AEI MS-50 instrument using the fast atom bombardment (FAB) method. The TG of complexes **1** and **3** was carried out with a Mettler Toledo Star system and Perkin-Elmer 7 series thermal analysis system, respectively. The UV spectra were recorded at 25 °C on a Shimadzu UV-2501PC spectrophotometer. CD spectra were recorded at 25 °C on a JASCO-20C automatic recording spectropolarimeter. The oxidation potential was detected on a Model 283 potentiostat/galvanostat with DMF as the solvent. Fluorescence spectra were recorded at 25 °C on a F-4500 spectrofluorometer with excitation and emission slits of 2.5 nm. The oligomers of ethylene were analyzed on a GC-MS (Shimatsu GC/MS-QP5050A) spectrometer.

Synthesis of 1-[(5-Methyl-2-furyl)methylene]-2-(5-methyl-2-furyl)benzimidazole (L1). A solution of anhydrous methanol (10 mL) containing 5-methylfuraldehyde (2.456 g, 22.3 mmol) and *o*-phenylenediamine (1.211 g, 11.2 mmol) was added to a three-necked flask, and the resultant mixture was stirred at 30−40 °C for 20 h under a nitrogen atmosphere. Most of the solvent was removed under reduced pressure, and then the residue was purified on a silica chromatography column with diethyl ether/petroleum ether (5:1) as eluent to give 1.96 g (60% yield) of **1** as a white powder. FAB-MS: *m*/*z* 293 [$M^+ + H$]. ^{1}H NMR (300 MHz, $CDCl_3$, 25 °C, TMS): δ 7.80−7.76 (m, 1H), 7.52−7.48 (m, 1H), 7.30−7.26 (m, 2H), 7.09 (d, 2H), 6.21 (d, 1H), 6.14 (d, 1H), 5.54 (s, 2H), 2.47 (s, 3H), 2.23 (s, 3H). ^{13}C NMR (300 MHz, $CDCl_3$, 25 °C, TMS): δ 154.5, 152.4, 147.7, 144.4, 143.4, 143.0, 135.6, 122.9, 122.7, 119.6, 113.9, 110.0, 109.2, 108.2, 106.4, 41.8, 13.9, 13.6.

Synthesis of Dichlorobis[1-((5-methyl-2-furyl)methylene)-2-(5-methyl-2-furyl)benzimidazole]cobalt (Complex 1). 1-[(5-Methyl-2-furyl)methylene]-2-(5-methyl-2-furyl)benzimidazole (0.3483 g, 1.2 mmol) was added to a solution of anhydrous $CoCl_2$ (0.0775 g, 0.6 mmol) in ethanol (10 mL), and the solution was stirred for about 10 h. The blue precipitate was collected by filtration, washed with diethyl ether, and dried under vacuum to yield 0.40 g (94%) of complex **1**. Anal. Calcd for $C_{36}H_{32}O_2N_2{\cdot}CoCl_2$: C, 60.52; H, 4.51; N, 7.84. Found: C, 60.19; H, 4.37; N, 7.78.

Synthesis of Dichlorobis[1-((5-methyl-2-furyl)methylene)-2-(5-methyl-2-furyl)benzimidazole]copper (Complex 2). Using a procedure similar to that described in the synthesis of complex **1**, the reaction of **L1** (0.1993 g) with $CuCl_2{\cdot}4H_2O$ (0.0666 g) gave 0.19 g (81.5%) of complex **2** as an orange powder. Anal. Calcd for $C_{36}H_{32}O_2N_2{\cdot}CuCl_2$: C, 60.13; H, 4.49; N, 7.79. Found: C, 60.08; H, 4.48; N, 7.53.

Synthesis of Dichlorobis[1-((2-furyl)methylene)-2-(2-furyl)benzimidazole]cobalt (Complex 3). Using a procedure similar to that described in the synthesis of complex **1**, the reaction of **L2** (0.1533 g) with $CoCl_2$ (0.0377 g) gave 0.18 g (94.2%) of complex **3** as a blue powder. Anal. Calcd for $C_{36}H_{32}O_2N_2{\cdot}CoCl_2$: C, 58.38; H, 3.67; N, 8.51. Found: C, 58.34; H, 3.54; N, 8.34.

Polymerization of Ethylene. Polymerization runs were performed at constant monomer pressure in a stainless steel autoclave (100 mL) equipped with a Julado ATS-3 temperature-controlling unit and magnetic stirrer. During polymerization, the partial pressure of the ethylene was kept constant by an electronic controlling system.

Toluene (60 mL) and MAO were introduced into the nitrogen-purged reactor. Once the polymerization temperature was reached, the vessel was charged with ethylene to an appropriate pressure. Polymerization was commenced by adding the catalyst recursor into the reactor. After the appropriate period of time, polymerization was quenched by draining the contents of the vessel into cold HCl-acidified ethanol, and the upper toluene phase was collected for GC-MS.

X-ray Crystal Structure Analyses. The crystals of complexes **1**−**3** suitable for X-ray crystallography were grown by slow evaporation of their ethanol solutions. The intensity data of complexes **1** and **2** were collected on a Bruker SMART diffractometer and complex **3** on a Rigaku R-AXIS RAPID imaging plate diffractometer, with graphite-monochromated Mo Kα (λ = 0.710 73 Å) radiation at 293 ± 2 K. The crystal structure was solved by direct methods and refined by employing full-matrix least squares on F^2, using the SHELXL97 package.[18] Crystallographic data have been deposited with the Cambridge Crystallographic Data Center as CCDC Nos. 173036, 173035, and 183921 for complexes **1**−**3**. Copies of the data can be obtained on application to the CCDC, 12 Union Road, Cambridge CB21EZ, U.K. (http://www.ccdc.cam.ac.uk).

Acknowledgment. We are grateful to the Chinese Academy of Sciences for financial supports under "One Hundred Young Talents" and Core Research for Engineering Innovation Grant No. KGCX203-2. W.H.S. thanks Prof. Gerhard Erker of Münster University and the Alexander von Humboldt-Stiftung.

Supporting Information Available: Unit cell and packing diagrams and tables of crystal data, atomic coordinates, bond lengths and angles, anisotropic displacement parameters, and hydrogen coordinates for complexes **1**−**3**. This material is available free of charge via the Internet at http://pubs.acs.org.

OM020370R

(15) Burley, S. K.; Petsko, G. A. *Science* **1985**, *229*, 23.
(16) Brömme, D.; Bonneau, P. R.; Purisima, E.; Lachance, P.; Hajnik, S.; Thomas, D. Y.; Storer, A. C. *Biochemistry* **1996**, *35*, 3970.
(17) Burmistrov, S. I.; Sannikova, V. M. *Khim. Geterotskl. Soedin.* **1981**, *6*, 816.
(18) Sheldrick, G. M. SHELXTL, Version 5.1; Bruker Analytical X-ray Instruments Inc., Madison, WI, 1998.